ACCOUNTS OF CHEMICAL RESEARCH

VOLUME 5 NUMBER 12 DECEMBER, 1972

MO Following: the Molecular Orbital Counterpart of Electron Pushing

HOWARD E. ZIMMERMAN

University of Wisconsin, Madison, Wisconsin 53706

Received April 24, 1972

During the last two decades organic reaction mechanisms have often been described using the technique of "electron pushing," this based on qualitative resonance reasoning.

The last decade has seen increasing use of MO theory. Attention has been focussed on *energy* changes along the reaction coordinate. The forms of the MO's, when available, have primarily been used to define symmetry and thus allow construction of correlation diagrams. But here it has been necessary that symmetry be maintained during a reaction[1] or that there be a cyclic orbital array which can be categorized as Hückel or Möbius.[2,3] Where no symmetry exists and where a simple orbital array cannot be discerned, MO discussion of the reaction has been confined to perturbation approaches which examine the energy of the highest occupied MO with the assumption that this is controlling.[4]

The present paper describes methods of following the *form* of MO's during a reaction. Such a treatment is the MO counterpart of electron pushing and is aptly termed "MO Following." The methods are capable of dealing with reactions lacking the symmetry to construct correlation diagrams by the methods of the literature while still being able to handle symmetric systems. Similarly, MO Following methods can cope with orbital arrays not simply described as Hückel or Möbius in the treatment we delineated some 6 years ago.[2]

Following the form of the MO's during reaction often allows insight into the factors making a reaction allowed or forbidden. Then one can discern what molecular geometric changes will minimize reaction forbiddenness.

Howard E. Zimmerman is a native of Connecticut. During World War II, he was in the U. S. Armored Corps in Europe. He received his B.S. and Ph.D. from Yale University in 1950 and 1953, respectively, and after a year of postdoctoral study at Harvard with R. B. Woodward he joined the faculty at Northwestern University. In 1960 he moved to Wisconsin where he is Professor of Chemistry. His research has included the study of carbanion rearrangements, the synthesis and chemistry of barrelene and semibullvalene, the stereochemistry of ketonization of enols, the application of MO theory to organic reactions, the di-π-methane rearrangement, demonstration of meta transmission of electronically excited aromatics, and mechanistic and exploratory organic photochemistry.

The Method

Two basic approaches prove most useful. The first assesses the electronics of the reacting molecular system at half-reaction and, with the half-reaction MO's available, develops a correlation of reactant–transition state–product MO's. This correlation is based on continuity of nodal character with extent of reaction.[5]

A second approach uses perturbation theory to give the change in each reactant MO and in each product MO as one proceeds toward half-reaction.

Throughout the treatment one assumes that: (1) MO energies increase with increasing number of nodes (this is well known); (2) the nodal structure of MO's changes continuously and in linear or totally cyclic arrays of basis orbitals the number of nodes does not change; (3) in a linear system the nodes tend to remain symmetrically disposed about the center of the array; (4) in linear systems, MO's having the same parity (*i.e.*, evenness or oddness) of nodes tend not to cross; and (5) appreciable interaction between MO's as a consequence of new bonding occurs only where the two bonding portions have matching nodal character (note below); this interaction also leads to noncrossing of MO's. In this treatment it is noted that one pays attention to nodes between atomic as well as hybrid orbitals but not to nodes which occur within such a component orbital.

Application to 1,2 Rearrangements of Carbenes

The method is best illustrated with examples lacking

(1) R. B. Woodward and R. Hoffmann, *J. Amer. Chem. Soc.*, **87**, 395 (1965); *Angew. Chem., Int. Ed. Engl.*, **8**, 781 (1969).

(2) H. E. Zimmerman, *J. Amer. Chem. Soc.*, **88**, 1564 (1966); *Accounts Chem. Res.*, **4**, 272 (1971).

(3) The method of M. J. S. Dewar, *Tetrahedron Suppl.*, **8**, 75 (1966), arrives at the same conclusions regarding the $4N + 2$ and $4N$ systems by an independent and unrelated derivation using NBMO perturbation theory.

(4) (a) Note K. Fukui in "Molecular Orbitals in Chemistry, Physics and Biology," P. Löwdin and B. Pullman, Ed., Academic Press, New York, N. Y., 1964, p 513. (b) Highest occupied MO arguments are used for dealing with sigmatropic rearrangements as discussed by R. B. Woodward and R. Hoffmann, *J. Amer. Chem. Soc.*, **87**, 2511 (1965).

(5) The present treatment is described in part by H. E. Zimmerman and L. R. Sousa, *ibid.*, **94**, 834 (1972).

Table I

Summary of Nodal Characteristics of Selected Systems[7]

Molecule	Pictorial representation[a,b]	Schematic notation	Molecule	Pictorial representation	Schematic notation[c]
Butadiene	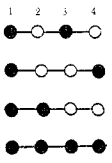	+1−2+3−4	"Benzyl"	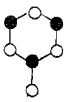	−(1-2)+4−5+6−7+8−9
		+1−2−3+4			
		+1+2−3−4			
		+1+2+3+4			
Cyclopropenyl	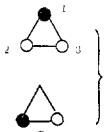	+1−2−3		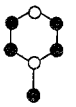	+(1-2)−4+5+6−7+8+9
		+2−3			
		+1+2+3			+5−6+8−9
Allyl	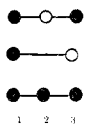	+1−2+3			
		+1−3			
		+1+2+3			
Cyclobutadiene	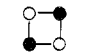	+1−2+3−4			+(1−2)−5+7−9
	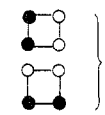	+1−2−3+4			+5+6−8−9
		+1+2−3−4			
	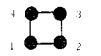	+1+2+3+4		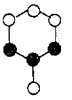	−(1-2)+4+5−6−7−8+9
Möbius cyclobutadiene	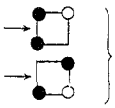	+1−3+4			
		+1−2+3			
	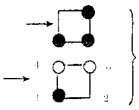	+1+2+3		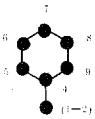	+(1-2)+4+5+6+7+8+9
		+1−3−4			

[a] Energies increase in each case going upward except for degenerate pairs marked ±. [b] → indicates top-bottom overlap. Note absolute signs of MO's are not meaningful (*e.g.*, +1−2+3 is as acceptable as −1+2−3). [c] α carbon labeled (1-2) and numbering corresponding to Figure 4.

symmetry. A first case involves the common, yet intriguing, 1,2 shift of hydrogen or an alkyl group to a carbene center to give an alkene.[6] Figure 1 depicts the gross orbital changes in this reaction together with an energy level diagram. The orbitals shown at the top of this figure are the basis set orbitals which are then combined to give the MO's. Below this are depicted the MO energy levels and how these correlate with one another. Finally, we concentrate in Figure 1c on MO 2 as an example and follow it as the reaction proceeds. Except for space limitations one would draw each MO transformation explicitly and follow the electron drift on reaction.

In getting the form of the MO's at partial reaction for this case, it is noted that these are butadienoid (*i.e.*, linear) in character, deriving from a linear array of four localized orbitals. For convenience, Table I gives this and some other simple MO's of interest.[7] Hence nodal properties can be properly assigned. Weighting of the basis orbitals in the MO's is not implied. Thus the notation (+1+2−3−4) merely implies that orbitals 3 and 4 have the reverse sign from 1 and 2 and that there is a node between orbitals 2 and 3. The notation then below each energy level in Figure 1b gives the nodal properties of that MO. Were the species in the center of Figure 1a butadiene itself, the MO's would have the same designations.

The form of the reactant and product MO's derives from the nature of the orbitals themselves as designated; thus, for example, σ_{23} is given as +2+3 and σ_{23}^* as +2−3. Similarly, π_{34} is +3+4 and π_{34}^* is +3−4.

It is assumed that the reactant and product MO's

(6) W. Kirmse, "Carbene Chemistry," Academic Press, New York, N. Y., 1964, p 52.

(7) (a) For the molecular orbitals of a variety of systems of interest note A. Streitwieser, "Molecular Orbital Theory For Organic Chemists," Wiley, New York, N. Y., 1961. (b) For benzyl MO's see "Dictionary of π-Electron Calculations," C. A. Coulson and A. Streitwieser, Ed., W. H. Freeman and Co., San Francisco, Calif., 1965, p 184. We note that the MO's of the benzylic species under discussion will differ quantitatively but not qualitatively from benzyl itself.

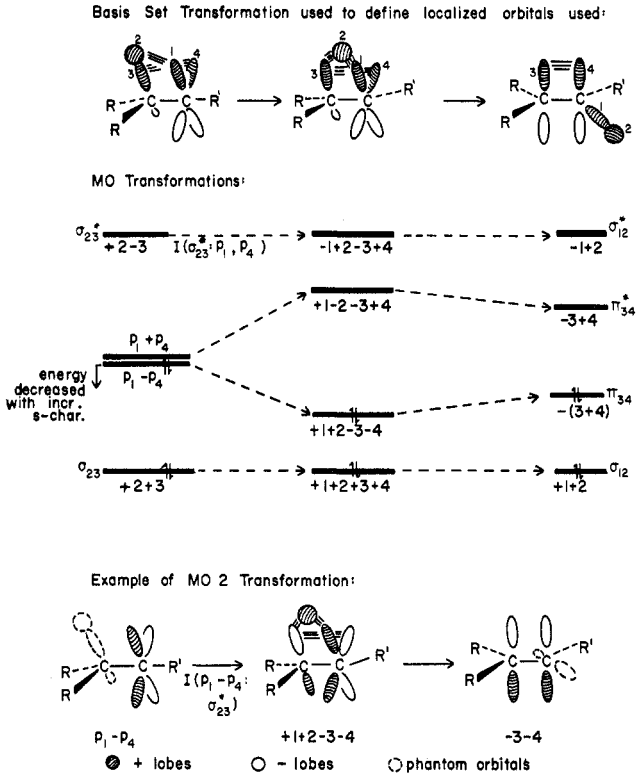

Figure 1. (a) Basis set transformation; (b) MO correlations; (c) MO 2 transformation.

are relatively localized and can be categorized as purely σ, π, etc. However, as the molecule deforms itself towards half-reaction geometry, the MO becomes more delocalized. Thus, σ_{23} picks up +1+4 character; similarly, σ_{23}^* picks up −1+4 character.

What new character is picked up by a reactant MO can be determined by the MO with which it correlates. The correlations are made with the assumption that nodal character tends to persist. Thus σ_{23} has the form +2+3 (*i.e.*, no node between orbitals 2 and 3) and MO 1 but not MO 2 of the half-reacted species has the same parity and correlates with σ_{23}. The new character picked (*i.e.*, added in) by a MO derives from other MO's of the system. How to decide which other MO's mix in is described further below.

In the reactant, p orbitals are arbitrarily shown at the carbene center although it is known that there is added s character. Since it will be desired to know which p orbitals are admixed with the s orbital (*vide infra*), no s character is utilized at this point in construction of the diagram. Also, although one could use p_1 for one level and p_4 for the other, it is better to use $p_1 + p_4$ and $p_1 - p_4$ linear combinations, since it is clear from MO's 2 and 3 of half-reacted species that these levels pick up both 1 and 4 character. Any linear combination of p_1 and p_4 will be equally acceptable for starting orbitals, however.

Then it is seen that $p_1 - p_4$ correlates with MO 2 of the half-reacted species since 1+2−3−4 has opposite signs for p_1 and p_4. Similarly, $p_1 + p_4$ transforms itself into the antibonding MO 3 of half-reacted species.

Another way to obtain information about the change in MO's with bonding is to use first-order perturbation theory. Thus each MO of reactant incorporates some of the other reactant MO's as the reaction proceeds. The rule for getting the resulting MO is to add each other MO to the one under consideration using an admixture factor Q given by the quotient in eq 1. The numerator is proportional to the overlap (S_{ko}) of the MO (o) under consideration with the MO (k) being added. But only newly bonding orbitals are included in considering the inter-MO overlap. The new overlap S_{ko}^{new} may be plus (*i.e.*, ++ or −−) or minus (*i.e.*,

$$Q_k = cS_{ko}^{new}/(E_k - E_o) \qquad (1)$$

+− or −+). The denominator is positive if one is mixing in a higher energy MO and negative with a lower energy MO. Therefore, if both numerator and denominator have the same sign, one adds in the MO contributed; if they are different, the MO being admixed is subtracted. Thus, c is a positive constant. This rule may be verbalized by saying that a given MO will steal part of another MO as a reaction proceeds if the change in overlap between the two MO's, considering all the sites of increased bonding, is nonzero; this really corresponds to the factor S_{ko}^{new}. It is seen that any MO character stolen is added in so that a lower energy MO has the maximum bonding and a higher MO doing any such stealing adds in the contributions to give maximum antibonding.

When this rule is applied to the perturbation of MO $p_1 - p_4$ one obtains terms only by interaction with the antibonding sigma orbital σ_{23}^*. This is seen qualitatively as follows. Thus $+p_1$ of MO $p_1 - p_4$ overlaps positively (*i.e.*, here ++) with the +2 of MO σ_{23}^* and the $-p_4$ portion of $p_1 - p_4$ overlaps with the −3 of σ_{23}^* and this too corresponds to a bonding interaction (*i.e.*, here −− overlap). Other attempted admixing of $+p_1 - p_4$ (*e.g.*, with σ_{23}) leads to one bonding overlap and one antibonding overlap, and no admixing results.

Alternatively, we can use eq 1 explicitly and come to the same conclusion. Accordingly, this interaction is designated $I(p_1 - p_4: \sigma_{23}^*)$ and leads to the correlations in Figure 1b. This interaction may be written as the sum of two interactions, namely $I(p_1: \sigma_{23}^*)$ and $I(-p_4: \sigma_{23}^*)$. These are of the ++ and −− variety, respectively, giving a positive numerator to the mixing coefficient. Since the orbital σ_{23}^* is above $p_1 - p_4$ in energy, the denominator of the mixing coefficient is also positive and the initial MO 2 (*i.e.*, $p_1 - p_4$) becomes $p_1 - p_4$ plus an increment of σ_{23}^* or approaches $p_1 - p_4 + 2 - 3 = +1+2-3-4$ as shown in Figure 1b. As noted above, other MO's do not admix with $p_1 - p_4$. This can be stated algebraically as well. For example, $I(p_1 - p_4: \sigma_{23}) = I(p_1: \sigma_{23}) - I(p_4: \sigma_{23}) = 0$. Analogously, $I(p_1 - p_4: p_1 + p_4) = 0$.

Similarly, one can arrive at the form of the other three reactant MO's as rearrangement begins. To correlate product and half-reaction MO's either one considers perturbation of the product MO's toward half-reaction by mixing in parts of other MO's either

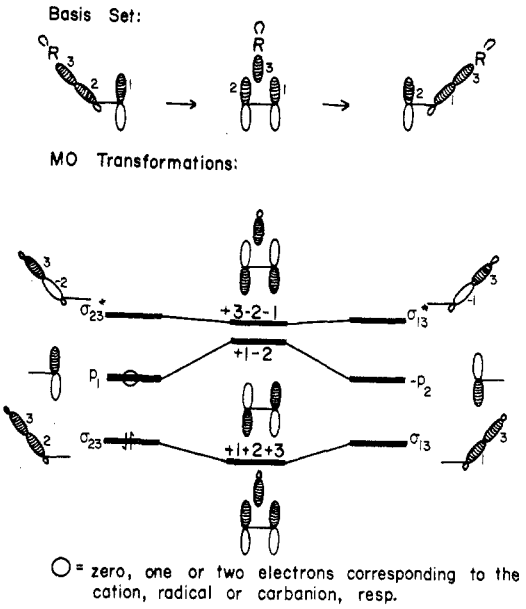

Figure 2. MO Following of 1,2 alkyl migrations.

by inspection or by use of eq 1 or one just compares nodal parity and connects levels of the same parity.

One interesting result from the correlation in Figure 1b is that the orbital $p_1 + p_4$ cannot be the orbital which is part of the sp^2 hybrid. If this were the case, this orbital would be lowered in energy and would be a bonding MO, containing an electron pair at the onset of reaction, and would become antibonding as the reaction proceeded. Such reactions are forbidden. The combination $p_1 + p_4$ is a vertically oriented (*i.e.*, in the plane of the paper of Figure 1) orbital with its plus lobe aimed toward the top of the page. This puts both the sp^2 hybrid and the R′ group in the plane of the paper; the forbiddenness then is understandable since a 90° twisted ethylenic bond is being generated.

What is needed is for the $p_1 - p_4$ orbital to pick up the s character; this means that this orbital is lowered in energy and becomes sp^2. Then all the bonding reactant orbitals remain bonding. Since $p_1 - p_4$ is a horizontal orbital (*i.e.*, perpendicular to the paper), the sp^2 hybrid and the group R′ remain horizontal during the allowed reaction.

Excitingly, one sees that with MO Following he can follow the drift of electron density, the motion of nodes, and the change of entire MO's as reactions continue. For example, in Figure 1c one notes that in MO 2 the carbene carbon orbitals are primarily weighted in reactant. But as the reaction proceeds, electron density diffuses to all four orbitals with a node between orbitals 2 and 3. As product is reached, the bonding ethylenic orbital is generated with a negative sign.

Other Examples

1,2 Migrations. Some years ago the MO treatment of 1,2 carbon to carbon migrations was discussed by Zimmerman and Zweig.[8,9] Energy level diagrams

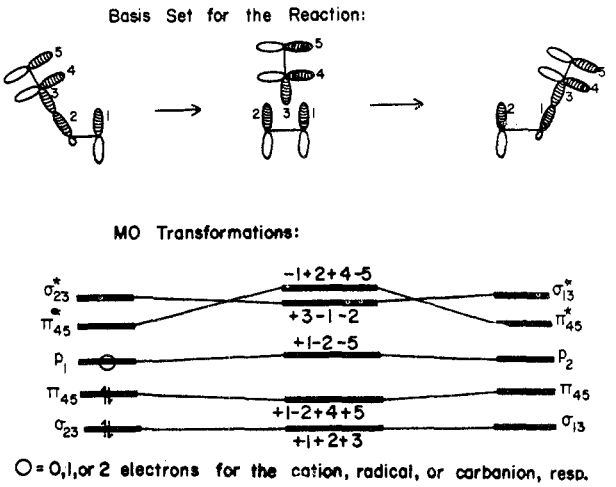

Figure 3. 1,2 vinyl shift.

were drawn for reactant, product, and half-reacted species, and the correlation of these levels was noted. It was also pointed out that where a bonding MO bearing electrons becomes antibonding during a reaction, that reaction will be energetically very unfavorable. This seems to be the first example of the use of correlation diagrams and of the concept of forbiddenness.

However, these early correlation diagrams were obtained by computer calculation of the MO's with geometries varying along the reaction coordinate; such an approach is hardly convenient for the organic chemist.

The same correlation diagrams can be readily obtained by inspection using MO Following techniques. The case of a 1,2 alkyl migration is discussed first and is outlined in Figure 2. Here we obtain the half-reaction MO's from knowledge of the form of a triangular orbital array. Or, using perturbation theory we see that $I(\sigma_{23}: p_1) \rightarrow \sigma_{23} + p_1 = +1+2+3$. Similarly, $I(p_1: \sigma_{23}, \sigma_{23}^*) \rightarrow p_1 - \sigma_{23} + \sigma_{23}^* = p_1 - 2 = +1-2$. Thus p_1 interacts both with σ_{23} and σ_{23}^*; the $-\sigma_{23}$ results since p_1 is interacting with a lower energy orbital. We note that, in the combination $-\sigma_{23} + \sigma_{23}^*$ (*i.e.*, $-(+2+3) + (-2+3)$), orbitals cancel and -2 is left. Analogously, $I(\sigma_{23}^*: p_1) \rightarrow \sigma_{23}^* - p_1 = -2+3-1$. In correlating the half-reaction MO's with product MO's it is convenient to consider perturbation of the latter toward half-reaction; this gives the MO changes shown. The correlation diagram is the one obtained by computer by us earlier.[8]

Thus, p_1 is seen to become antibonding on reaction, and the carbanion and free-radical rearrangements, where this MO is occupied, are energetically difficult. In looking at the reason for the energetics, it is seen that p_1 becomes antibonding (*i.e.*, $p_1 - p_2$) as it is transformed gradually into $-p_2$. Electron density can leak from C-1 to C-2 only with intermediate 1,2-antibonding.

Quite similarly, the MO's for 1,2 vinyl and 1,2 phenyl shifts may be followed. Figure 3 details the

(8) H. E. Zimmerman and A. Zweig, *J. Amer. Chem. Soc.*, **83**, 1196 (1961).

(9) These calculations have been confirmed with modified parameters by N. F. Phelan, H. H. Jaffé, and M. Orchin, *J. Chem. Educ.*, **44**, 626 (1967).

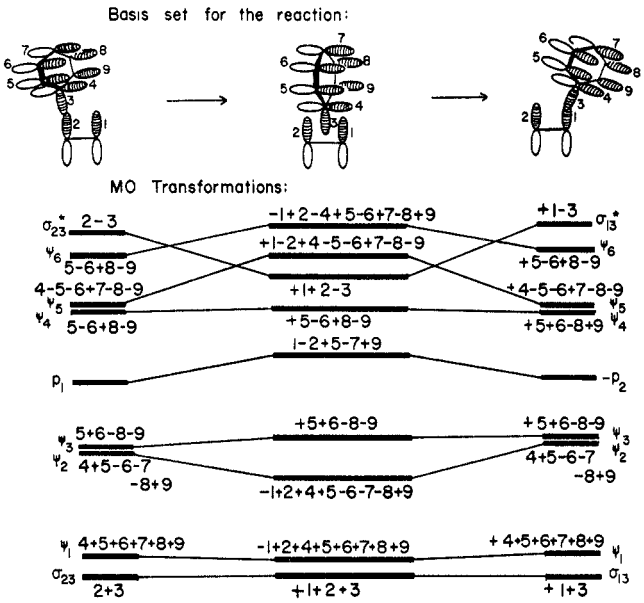

Figure 4. 1,2 phenyl migrations.

1,2-vinyl shift case. This case is most readily derived using the method of maximum similarity of MO's for correlation. The half-reaction MO's of the vinyl bridged species can be seen to consist of (a) a set symmetric with respect to a plane through orbitals 3, 4, and 5 and perpendicular to the paper and (b) an antisymmetric set. The former cannot include p_4 and p_5 (which are inherently antisymmetric) and derive from $(p_1 + p_2)$ and p_3. Admixing of these two orbitals gives $+1+2+3$ and $+3-1-2$ (*i.e.*, the sum and difference). The antisymmetric group orbitals are $(p_1 - p_2)$, p_4, and p_5. This is a linear array and therefore leads to three allyl-like MO's, namely $+1-2+4+5$, $+1-2-5$, and $+1-2-4+5$. In writing down these three orbitals using the allyl entry of Table I, we use $+1-2$ as one basis orbital at one end of the molecule. Furthermore, unlike Table I, we take 4 as the orbital in the middle and 5 as the other end one. With $p_1 - p_2$ being antibonding all MO's are raised in energy, including the central one which ordinarily would be nonbonding.

The correlations between half-reaction and reactant and product MO's derive from assumption of gradual and continuous change in nodal character.

If one applies the perturbation approach to a case such as this, one finds some extraneous basis orbitals in the MO's derived. Thus $I(\sigma_{23}: \pi_{45}, p_1, \pi_{45}^*) \rightarrow +1+2+3-4$, and, especially in view of the symmetry of $+1+2+3$, it is seen that -4 is extraneous. The problem is that the perturbation approach really gives weightings developed early in the migration and these differ somewhat from the mid-reaction MO's. The simplest approach is to annihilate all parts of the derived MO's not conforming to molecular symmetry and to that of the major portion of the derived MO.

We note that p_1—the MO which bears one electron in the 1,2 radical shift, two electrons in the 1,2 carbanion shift, but none in the carbonium case—correlates with the antibonding MO $+1-2-5$. This is the same kind of situation found for the 1,2 alkyl shift. However, presently the MO $+1-2-5$ is only slightly antibonding due to the distribution of electron density from the antibonding center $+1-2$ onto carbon 5. This explains the ability of vinyl to migrate in carbanions and free radicals. Thus, MO Following reveals the effect allowing 1,2 vinyl radical and carbanion rearrangements; the revelation is in terms of minimizing an unfavorable electron density drift leading to antibonding rather than mere statement of unfavorable energy.

The case of the 1,2 phenyl shift is no more difficult (note Figure 4). Here the reactant MO's are those of the p orbital at C-1, the bonding and antibonding orbitals of the σ bond holding the phenyl group to C-2, and the benzenoid orbitals of the migrating phenyl. The product MO's are obtained similarly. For the half-reaction MO's, it is simplest to note that there are two group orbitals which are symmetric with respect to the plane of the aromatic ring, namely $+1+2$ and $+3$. These admix in plus and minus combinations to give the MO's $+1+2+3$ and $+1+2-3$ as shown in Figure 4. The other seven MO's are easily written down by inspection once one realizes that they constitute a benzyl-like array; the only difference from benzyl[7b] (note Table I) itself is that the exocyclic basis orbital is $+1-2$ rather than a single p orbital. Thus, the antisymmetric basis set MO's are benzyl-like but have an orbital which is higher in energy than the usual nonbonding p orbital of benzyl.

Interestingly, it is seen that the MO situation is quite similar for phenyl migration compared to vinyl migration in that again there is a slightly antibonding MO which is generated at half-reaction and which is occupied in the free-radical and carbanion rearrangements. The difference for phenyl migration is quantitative in that, due to weightings of p orbitals 5, 7, and 9, there will be lower election density in orbitals 1 and 2 compared with the vinyl case. Due to this drainage of electron density away from the $+1-2$ antibonding orbital pair, the radical and carbanion rearrangement reactions presently are less forbidden than for the vinyl migration cases.

Another related point is that orbital 7 is weighted in this MO and thus any substitution at this point by electron-deficient conjugating groups should still further facilitate the aryl migration.

Carbene Additions to π Bonds. A simple and further illustrative case involves the addition of methylene to alkenes. The correlation diagram is given in Figure 5a. As in the carbene rearrangement case above, the one-carbon fragment is initially considered as having only two p orbitals with the intention of adding s character to one of these subsequently. The real question is which p orbital requires s character and begins with two electrons for the reaction to be allowed. The reaction utilizes a total of four delocalized electrons, two in the initial π bond and two in the carbene.

The half-reaction MO's are seen to be of the linear type and have the usual butadienoid nodal properties.

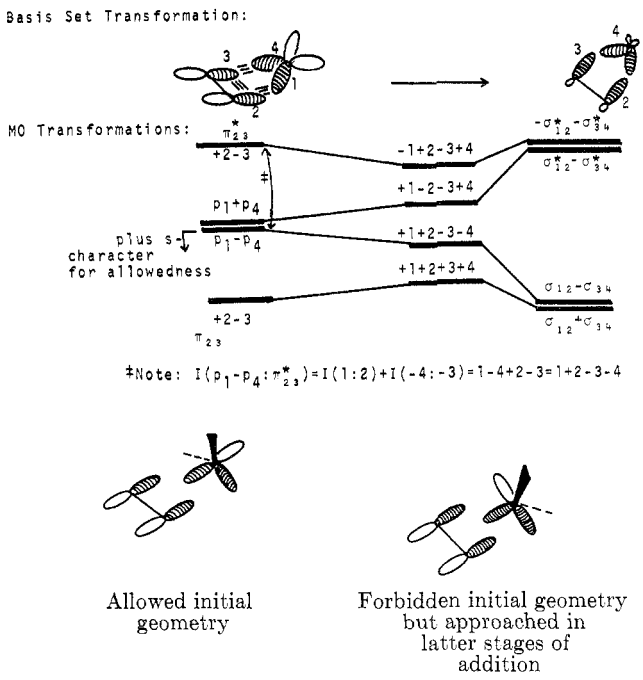

Figure 5. (a, upper) addition of methylene to alkenes; (b, lower) allowed and forbidden initial geometries for carbene addition to an alkene.

Thus, if we were to use pure p_1 as one starting orbital and pure p_4 as the other, these quickly admix in plus and minus combinations, since each MO develops weightings of all four orbitals. For this reason it is convenient to use $p_1 + p_4$ and $p_1 - p_4$ as the initial two p orbitals; as noted, this character develops quickly anyway.

The alternative approach to this correlation diagram is use of the perturbation method. Thus, it is readily determined that the initial MO $p_1 - p_4$ interacts only with π_{23}^*. The result is $I(p_1 - p_4: \pi_{23}^*) = I(1: 2) + I(-4: -3) = +1-4+2-3 = +1+2-3-4$. Other potential interactions of $p_1 - p_4$ are readily found to be zero. Finally, in analogous manner the change in the other three initial molecular orbitals, on perturbation toward half-reaction, can be shown to give the same results as derived by use of nodal properties.

As Figure 5a reveals, it is the $p_1 - p_4$ combination which correlates with a bonding product MO and which therefore is the orbital which should be initially occupied for the reaction to be allowed. But $p_1 - p_4$ can be seen to be a p orbital which is parallel to the C-2 to C-3 axis, and it is this orbital which then becomes sp^2. The other orbital which is vacant is $p_1 + p_4$; this is a pure p orbital directed between orbitals 2 and 3. This geometry certainly makes intuitive sense since with the vacant p orbital of the carbene attacking the π system rather than the occupied sp^2 orbital there is a cyclic Hückel[2] array of three orbitals containing two delocalized electrons; this intuitive approach though neglects the sp^2 orbital as an approximation.

Hence, the treatment of the carbene addition to an alkene leads to the prediction that, for an allowed reaction, the initial geometry shown on the left in Figure 5b is required, while the initial geometry shown on the right in Figure 5b leads to a forbidden reaction. On

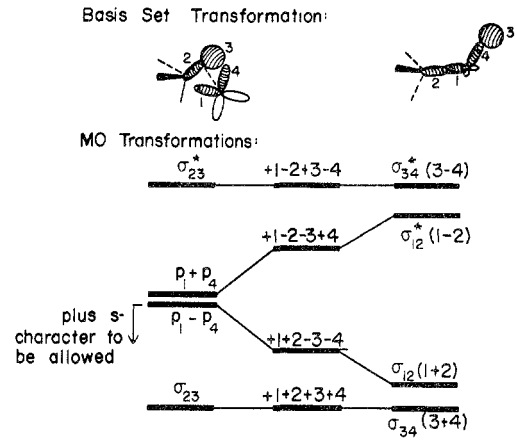

Figure 6. Insertion of methylene into a C–H bond.

inspecting the product MO's, we see that the orientation has been modified with formation of two equivalent σ bonds, σ_{12} and σ_{34}, and the initially forbidden orientation eventually becomes attained. This results from rehybridization of orbitals 2 and 3 with injection of s character in the orbital resulting from transformation of π_{23}, and a twisting of the CH_2 moiety occurs in the latter portion of the reaction. Accordingly, not only initial geometry is predicted by MO Following but also the change in geometry along the reaction coordinate; this does agree with the detailed literature calculations.[10a]

Carbene Insertion into C–H Bonds. This treatment is exactly parallel to the addition of a carbene to a π bond, except that here a σ bond in reactant substitutes for the π bond of the previous example. The correlation diagram is shown in Figure 6. Again, for allowedness, we need to keep the four delocalized electrons in bonding MO's. Since two nonequivalent σ bonds result in this reaction, the product MO's are nondegenerate and are pictured as separate σ bonds, that is, C–H and C–C. In the previous example of addition to the π system, two equivalent σ bonds resulted, and it was permissible to replace the separate σ bonds (there both C–C) by linear combinations. Such linear combinations conform better to the arrays present during reaction, and there is some advantage for clarity in using these where the product MO's are degenerate. Finally, in connection with the insertion reaction, the present MO Following treatment agrees with calculation.[10b]

Sigmatropic Rearrangements. One limitation in understanding 1,*n* sigmatropic rearrangements is that there is no symmetry element maintained throughout the reaction and thus symmetry cannot be used to construct correlation diagrams. Most frequently a perturbation argument is used dealing only with the highest occupied MO's of each of two fragments.[4b] MO Following is not subject to this limitation.

Figure 7 provides the example of a 1,3-suprafacial sigmatropic rearrangement of a hydrogen while Figure 8 shows the corresponding 1,3-antarafacial migration.

(10) (a) R. Hoffmann, *J. Amer. Chem. Soc.*, **90**, 1475 (1968); (b) R. D. Dobson, D. M. Hayes, and R. Hoffmann, *ibid.*, **93**, 6188 (1971).

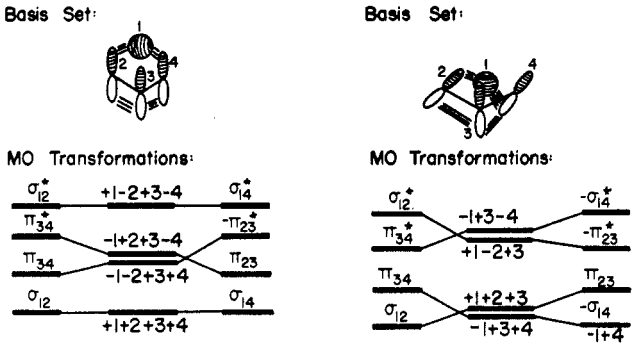

Figure 7 (left). 1,3-Suprafacial hydrogen shift.
Figure 8 (right). 1,3-Antarafacial hydrogen migration.

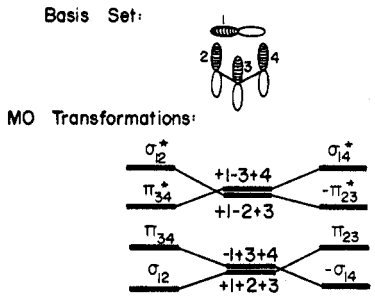

Figure 9. 1,3-Suprafacial sigmatropic p-orbital shift with inversion.

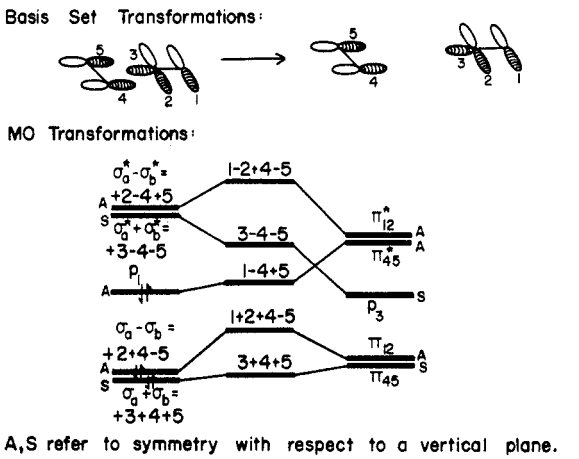

Figure 10. The cheletropic disengagement of carbon monoxide from cyclopropanone.

To obtain the half-reaction MO's in these cases one needs the form of the MO's for a Hückel[2] cyclic array, as present in the suprafacial migration, and for the Möbius array[2] present in the antarafacial half-reaction species of Figure 8. The former are cyclobutadienoid and easily formulated as in Figure 7. The form of the latter[11] is given in Table I and used in Figure 8. Again the assumption is made that the MO's which correlate are those with minimum disturbance of their nodal characteristics.

An alternative approach to obtaining the half-reaction MO's in Figure 8 is to use the perturbation treatment. If we do this, we find that among the reactant MO's σ_{12} interacts only with π_{34}^* and π_{34} interacts only with σ_{12}^*. The half-reaction MO's are obtained then from each reactant and each product MO. For example, $I(\sigma_{12}: \pi_{34}^*) = I(1+2: 3-4) = \sigma_{12}+3-4 = +1+2+3-4$. Similarly, $I(\pi_{34}: \sigma_{12}^*) = I(3+4: 1-2) = \pi_{34}-1+2 = -1+2+3+4$. There is one subtlety to be noted, however. This occurs when the half-reaction MO derived from a product MO differs from the form obtained from the reactant MO. For example, perturbing product MO σ_{14} gives $I(\sigma_{14}: \pi_{23}^*) = I(1-4: 2+3) = \sigma_{14}+2-3 = +1-4+2-3$. This is seen to be the negative of the orbital derived from reactant MO π_{34} except for term 2 which does not agree in sign. This indicates that this term is actually zero; the perturbation approach is simplistic enough that one has to be alert to getting different linear combinations when a degenerate pair is approached from different directions and to such extra terms.

These rearrangements involve four delocalized electrons, and one can see that the 1,3-suprafacial hydrogen shift leads one of two occupied MO's to become antibonding and the reaction is thus forbidden. The 1,3-antarafacial shift keeps occupied MO's bonding and is allowed.

A related example is that of a 1,3-sigmatropic rearrangement suprafacially but with inversion of configuration of the migrating carbon atom. This is depicted in Figure 9. Again it is seen that the array is Möbius-like, and the half-reaction MO's have the typical form (note Table I) for such cyclic systems. Since two bonding MO's correlate with two bonding MO's of product, a closed-shell reaction will nicely accommodate four electrons, the number in reactant. Therefore the reaction is allowed.

Cheletropic Disengagement Reactions. One example of interest is the cheletropic disengagement of carbon monoxide from cyclopropanone. While this reaction has a plane of symmetry and could be treated by the usual methods, use of MO Following provides a comparison.

The correlation diagram is given in Figure 10. The system has six electrons delocalized. The reactant and product MO's are written by inspection using the starting and product π orbitals plus the nonbonding oxygen orbital labeled p_1. For starting σ orbitals it is convenient to select the sum and difference orbitals $\sigma_a \pm \sigma_b$, where these are the bond orbitals, since these orbitals turn out to conform to the symmetry of the mid-reaction MO's and correlate nicely with them. The mid-reaction MO's interestingly are the same set as in the 1,2 vinyl migration discussed earlier. The cor-

(11) H. E. Zimmerman, unpublished. The form of Möbius MO's most conveniently used is trigonometric. Thus, the LCAO MO coefficients are given by $C_{rk}^{+} = (2/N)^{1/2} \cos [(2k+1)\pi r/N]$ and $C_{rk}^{-} = (2/N)^{1/2} \sin [(2k+1)\pi r/N]$, where k refers to the MO and increases from 0 to $N/2 - 1$ or $(N-1)/2$ with increasing energy, for N even or odd, respectively (note highest MO redundancy for N odd), r gives the basis orbital number and runs from 1 to N, and N gives the number of orbitals in the system. Since the MO's come in degenerate pairs except possibly for a highest energy one, the + and − refer to the two degenerate MO's of each energy. The linear combinations obtained in this fashion for Möbius cyclobutadiene give coefficients: 0.5, 0, −0.5, −0.707 and 0.5, 0.707, 0.5, 0 for the lowest energy degenerate pair; here the basis set overlaps +− between the terminal atoms. The antibonding coefficients are: −0.5, 0, 0.5, −0.707 and 0.5, −0.707, 0.5, 0. This is seen to correspond to the form used presently.

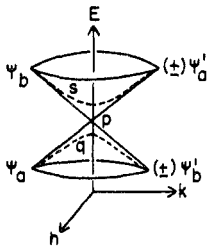

Figure 11. MO energies of potentially degenerate pair as a function of energy difference, k, and interaction element, h. Here p is the crossing point, ——— gives the crossing route, and ---- gives the noncrossing route.

relations in the present instance derive as usual from nodal properties but also could be derived from symmetry with respect to a plane bisecting and perpendicular to σ bond 4,5 and p orbitals 1 and 2. The symmetry derived correlation, using the method of Woodward and Hoffmann, proves the same as the one obtained by MO Following; both of these can be seen to predict a forbidden ground state process.

Near Crossings; Minimization of Forbiddenness. One further point of considerable interest deals with the question of whether the pathways for forbidden reactions really are properly represented by MO crossings and degeneracies along the reaction coordinate. In fact, for most molecular species, such degeneracies are split by molecular distortions with net energy lowering, this being the Jahn–Teller effect.[12a] Thus, a better representation of the surface available to two MO's capable of crossing is given in Figure 11. This depicts the nature of the energy surface of a pair (Ψ_a and Ψ_b) of MO's close to the point of crossing.[12b] As noted by Herzberg and Longuet-Higgins[12b] and Teller,[12c] the surface consists of a double cone. The vertex is at p. The coordinate h is a measure of the amount of interaction between the MO's and k is a measure of their energy difference. If, due to different symmetry, for example, there is no interaction between the two MO's, then h is zero throughout, the correlation diagram is followed in the E–k plane and there is a crossing traversed at point p. This is the situation assumed thus far in MO Following.

However, this pathway is not necessarily the lowest energy one available and often is not. Thus, a pathway can be found in which the degeneracy is split by interaction (*i.e.*, $h \neq 0$) between the two MO's. With h non-zero, it is seen that the pathway utilized is the dashed one in Figure 11. Here the MO's proceed through points q and s and not through the conical vertex. If Ψ_a is the highest occupied MO of reactant, then this route does not involve an occupied MO becoming antibonding, although the approach to point p can be described as an "attempt to cross." It can be seen that as the interaction between MO's (*i.e.*, h) becomes larger, the reaction becomes less forbidden.

It can be shown[13] that in such pathways Ψ_a is converted into $-\Psi_b'$ and Ψ_b into Ψ_a' if h is positive (*i.e.*, an antibonding interaction between reactant MO's), or conversely that Ψ_a is converted into Ψ_b' and Ψ_b into $-\Psi_a'$ if h is negative (*i.e.*, a negative interaction energy, bonding). The sign changes are thus different than in the simple correlation diagrams and this is the reason for the (±) indicated next to the product MO's in Figure 11.

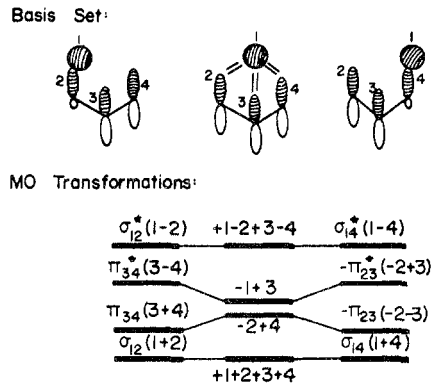

Figure 12. 1,3-Suprafacial hydrogen migration with inclusion of 1,3 overlap.

The near-crossing correlation diagrams are constructed using MO Following just as where we assumed no interaction and thus permitted crossing. This is readily demonstrated for examples already considered. Accordingly, the 1,3-suprafacial sigmatropic rearrangement described in Figure 7 above is reformulated in Figure 12. Here the degeneracy of highest bonding and lowest antibonding MO's is avoided by forcing h to become non-zero as the crossing is approached. This is accomplished by inclusion of appreciable 1,3 overlap. The correlations obtained for the bottom and top MO's are the same as in Figure 7. However, the correlations of MO's 2 and 3 differ. In the first place, originally we chose the nonbonding cyclobutadienoid MO's arbitrarily as 1+2−3−4 and 1−2−3+4. An equally acceptable combination would have been 1−3 and 2−4; these latter are seen to be the sum and difference of the first set. However, if we include the interaction between basis orbitals 1 and 3, the degeneracy is split and we no longer have a choice of which form to use. It is seen that the MO 1−3 has an antibonding interaction and has its energy raised once we include 1,3 overlap, while the MO 2−4 is unchanged. This leads to the splitting seen in Figure 12. Alternatively, we could have gotten this result by noting that the half-reaction array in Figure 12 is isoelectronic with 1,3-dehydrocyclobutadiene and obtained the form of its MO's.

It is seen that the correlation diagram differs in not having a crossing and also in having the second MO of product being the negative of the π_{23} obtained with

(12) (a) H. A. Jahn and E. Teller, *Proc. Roy. Soc., Ser. A*, **161**, 220 (1937); (b) G. Herzberg and H. C. Longuet-Higgins, *Discuss. Faraday Soc.*, **35**, 77 (1963); (c) E. Teller, *J. Phys. Chem.*, **41**, 109 (1937).

(13) H. E. Zimmerman, unpublished. Note: the two MO's are given by $\Psi^- = \cos(\theta/2)\Psi_1 - \sin(\theta/2)\Psi_2$ and $\Psi^+ = \sin(\theta/2)\Psi_1 + \cos(\theta/2)\Psi_2$, as given in ref 12b. Here $\cos\theta = k/(k^2 + h^2)^{1/2}$ and $\sin\theta = h/(k^2 + h^2)^{1/2}$. Therefore, in proceeding from reactant to product θ varies from 0 to 90° to 180° if h is positive and from 0 to −90° to −180° if h is negative during the reaction.

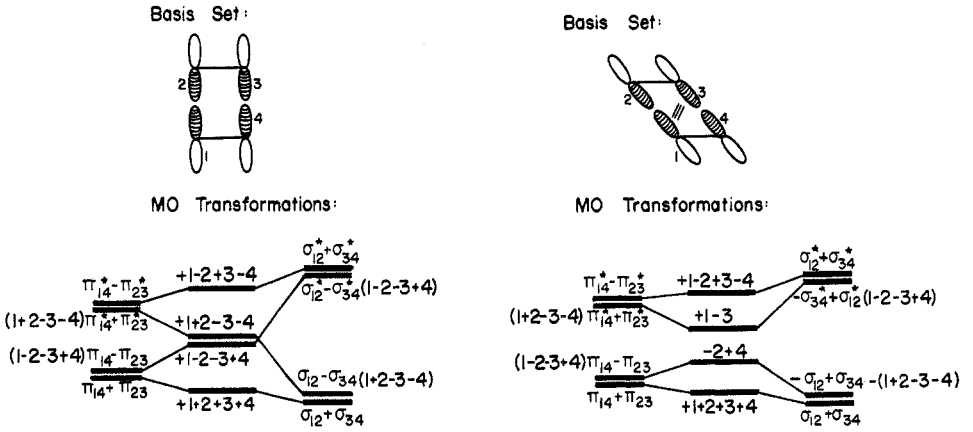

Figure 13. Crossing and noncrossing routes for ethylene dimerization (a, left; b, right).

crossing permitted. This type of correlation fits the generalization noted above, namely that, with an antibonding interaction between the two MO's being split (*i.e.*, 1+2−3−4 and 1−2−3+4; note that these overlap +−between orbitals 1 and 3), h is positive and the lower MO after the attempted crossing is derived from the higher MO before the crossing. Thus, $-\pi_{23}$ has a −3 component while π_{34}^* has a +3 weighting, and basis orbital 3 is the only part of π_{34}^* which survives in the second MO after the reaction.

In this case, the avoided crossing derives naturally from inclusion of overlap which is really present and which was artificially excluded previously for simplicity of discussion. However, one can find examples where introduction of interaction between MO's crossing has to derive from a geometric perturbation of the system.

One such example is the forbidden, four-center 2 + 2 symmetric addition of two ethylene molecules to give cyclobutane. The correlation diagram is characteristic of a forbidden reaction with crossing of MO's 2 and 3, as long as perfectly square geometry is maintained. This is true even when 1,3 and 2,4 overlap is included. Note Figure 13a. However, if parallelogram geometry is employed for the reaction, then there is additional 1,3 overlap between basis orbitals which is greater than 2,4 overlap. This leads to splitting of MO's 2 and 3 as shown in Figure 13b. The reasoning is similar to that of the 1,3-sigmatropic rearrangement previoulsy discussed. We correlate MO's again by requiring continuity of sign for those parts of the MO remaining weighted as one proceeds along the reaction coordinate. We note that the correlation obtained by avoiding forbiddenness and the crossing is quite similar to that for the crossing route, except that, where there is splitting, the sign of the lower energy MO deriving from the split pair is the negative of the MO derived without splitting (*i.e.*, $\sigma_{12} - \sigma_{34}$ *vs.* $-\sigma_{12} + \sigma_{34}$). Thus the third MO of reactant is transformed into the second MO of product in both the crossing and noncrossing cases; however, in the latter case it is seen to be converted to its negative by traversing the route avoiding the conical vertex. That it is the lower (*i.e.*, $\sigma_{12} - \sigma_{34}$ or $-(1+2-3-4)$) which is formed negatively is expected on the basis of the previous discussion, since the interaction between the potentially crossing MO's is between basis orbitals 1 and 3 and is negative and antibonding between MO's 2 and 3 as given.

The conclusion which then derives from this discussion is that for the present reaction a distortion from square geometry for the half-reaction species is stabilizing. Of course, there is a limit to which stabilization can be obtained due to other adverse energy effects on distortion such as bond bending. Nevertheless, one can devise such perturbations in many cases which will minimize the reaction forbiddenness.

Conclusion

The general approach of MO Following is seen to allow one to focus attention on the molecular orbital effects which control the reaction energy deriving from electronic delocalization effects. Rather than leading blindly to predictions, MO Following allows insight into the factors controlling reaction allowedness and forbiddenness. While really not quite as simple as electron pushing, this MO treatment in fact parallels electron pushing in being qualitative but powerful.

Support of this research by the National Science Foundation, U. S. Army Research Office (Durham), and National Institutes of Health Grant GM-7487 is gratefully acknowledged.